

# A study of 2-azido-3,5-dichlorobiphenyl by nano- and picosecond laser flash photolysis and computational methods†

Nina P. Gritsan,<sup>\*a,b</sup> Dmitrii A. Polshakov,<sup>a</sup> Meng-Lin Tsao<sup>a</sup> and Matthew S. Platz<sup>\*a</sup>

<sup>a</sup> Department of Chemistry, The Ohio State University, Columbus, Ohio 43210.

E-mail: platz.1@osu.edu; Fax: 1 614 292 5151; Tel: 1 614 292 0401

<sup>b</sup> Institute of Chemical Kinetics and Combustion and Novosibirsk State University, 630090

Novosibirsk, Russia. E-mail: gritsan@kinetics.nsc.ru; Fax: 7 3832 342350; Tel: 7 3832 333053

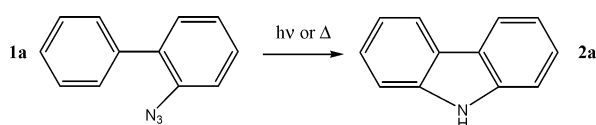
Received 7th April 2004, Accepted 4th May 2004

First published as an Advance Article on the web 13th May 2004

The dynamics of singlet 3,5-dichloro-2-biphenylnitrene and the products of its rearrangement were monitored by pico- and nanosecond laser flash photolysis and the results were consistent with the predictions of DFT and *ab initio* molecular orbital calculations.

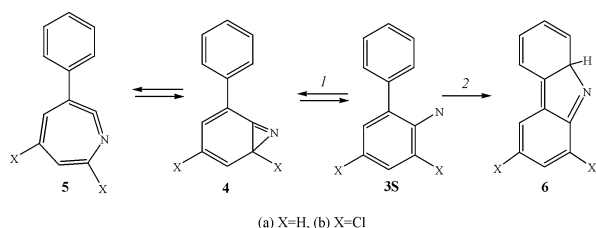
## Introduction

We have recently reported a study of the photochemistry of ortho-biphenyl azide (**1a**) using laser flash photolysis (LFP) methods.<sup>1</sup> It is well known<sup>2</sup> that photolysis and pyrolysis of **1a** produces carbazole (**2a**) (Scheme 1). It is one of the most synthetically useful photochemical reactions of aryl azides.



Scheme 1

The system is complicated by the fact that the key intermediate of this reaction, singlet ortho-biphenyl nitrene ( $X = \text{H}$ , **3Sa**), undergoes two processes, (1) and (2), at competitive rates, and that azirine formation is reversible (Scheme 2).<sup>1</sup>



Scheme 2

LFP of **1a** in fluid solution does not produce singlet nitrene **3Sa** as a detectable species on the nanosecond time scale. Instead, benzazirine **4a** and isocarbazole **6a** were observed immediately (<10 ns) after the laser pulse.<sup>1</sup>

The *ortho*-phenyl group directs azirine formation away from the substituent,<sup>3</sup> ortho-alkyl and fluorine substituents behave similarly.<sup>4</sup> Two *ortho*-methyl or halogen substituents can extend the lifetime of a singlet aryl nitrene by one or two orders of magnitude by retardation of azirine formation (process 1).<sup>4,5</sup> Substituents are not expected to influence the rate of formation of isocarbazole **6** (process 2). Thus, it seems reasonable to predict that replacement of the *ortho*-hydrogen of 2-biphenylnitrene with halogen ( $X = \text{Cl}$ ) might simplify the chemistry of the singlet 2-biphenylnitrene and allow straightforward study of

process 2, the formation of isocarbazole **6**. In addition, we have applied ultrafast transient absorption techniques to monitor the dynamics of singlet nitrene **3Sb** ( $X = \text{Cl}$ ) on the picosecond time scale at ambient temperature. Herein, we are pleased to report the results of our study.

## Experimental

### Laser flash photolysis: nanosecond time scale

A Nd:YAG laser (Spectra Physics LAB-150-10, 266 nm, 5 ns, 50 mJ) or XeCl excimer laser (Lambda Physik, 20 ns, 50 mJ, 308 nm) was used as the excitation light source. The spectrometer has been described previously.<sup>1,6</sup> Typically, solutions were prepared in dry spectroscopic grade solvents to an optical density (OD) of about 1.5–2.0 at the excitation wavelength (266 or 308 nm). The temperature was maintained at 77 K by means of boiling liquid nitrogen or varied over the range of 150–300 K by passing a thermo-stabilized nitrogen stream over the sample and held to within  $\pm 1$  K. In these experiments, a quartz cuvette was placed in a quartz cryostat. The sample solutions were changed after every laser shot, unless otherwise indicated.

### Picosecond pump-probe experiments

For detection of kinetics on the picosecond time scale, we used a pump-probe spectrometer.<sup>7</sup> A regenerative amplified, kHz repetition rate Ti:S laser system produces up to 20  $\mu\text{J}$  pump pulses with center wavelength 265 nm, using two Type I BBO crystals. Typical probe pulse energies used were 3–5  $\mu\text{J}$  at the sample. The pump beam was focused to a 0.6 mm diameter spot. Probe pulses between 370–750 nm were generated by focusing the laser fundamental in a water cell. Polarization of pump and probe were set to the magic angle ( $54.7^\circ$ ). After traversing the sample, the probe beam was passed through an  $f = 0.25$  m monochromator to isolate an approximately 10 nm portion of the continuum for single wavelength experiments.

Transient absorption spectra were recorded by scanning the monochromator. Since the total group delay between the shortest and the longest wavelength of the continuum is about 3 ps, it is not necessary to apply group delay ('chirp') correction to transient spectra recorded after 10 ps. The instrument response was approximately 220 fs (Gaussian full width at half-maximum, fwhm), which was determined by difference frequency mixing between the third harmonic and 10 nm portion of the continuum in a thin BBO crystal. To minimize the effects of photoproducts we prepared the sample in a large reservoir (1 L) with a concentration of 0.003 M. The sample solution was continuously circulating through the jet system as described.<sup>7</sup>

† Dedicated to Professor Hiroshi Masuhara on the occasion of his 60th birthday.

## Quantum chemical calculations

The geometries of the singlet and triplet states of 3,5-dichloro-2-biphenylnitrene (**3b**) were fully optimized at the CASSCF/6-31G\* (5D) level.<sup>8,9</sup> An (8,8) active space was employed for the calculation; the selected molecular orbitals were similar to those used in the calculation of unsubstituted phenylnitrene.<sup>10</sup> The dynamic electron correlation was included using CASPT2/6-31G\* (5D) calculations<sup>11</sup> with the CASSCF optimized geometries. During the CASPT2 calculations of **3Sb**, an intruder problem<sup>12</sup> was present as a low reference weight was obtained. This problem was solved by applying an initial 0.1 h level shift<sup>12</sup> prior to the CASPT2 calculations of **3Sb** and **3Tb**. Both CASSCF and CASPT2 calculations were carried out with a MOLCAS program (version 5.0).<sup>13</sup>

To compute the possible reaction pathways of the singlet nitrene, geometries of proposed reactive intermediates and transition states were fully optimized using the B3LYP<sup>14</sup> method with the 6-31G\* (6D) basis set. Vibrational frequencies were calculated to analyze the nature of the stationary points (minimum or transition state) and were used to account for ZPE differences. Single-point energies were then calculated using the B3LYP/6-311+G(2d,p) method<sup>15</sup> for B3LYP/6-31G\* optimized geometries. For the transition states connecting the open-shell singlet nitrene and a closed-shell intermediate, a standard DFT calculation fails to predict the chemistry properly. Thus, the broken symmetry DFT calculations (UB3LYP method with mixed HOMO and LUMO to destroy the spatial symmetry) were used for the calculations of these transition states. The calculated  $\langle S^2 \rangle$  values of these transition states were found to be small and to fall in the range of 0.04–0.28, except **TS<sub>3Sb-6b</sub>** in which the  $\langle S^2 \rangle$  value was very high ( $\approx 0.6$ ). Time dependent DFT (TD-DFT) calculations<sup>16</sup> were performed at the B3LYP/6-31G\* level. All DFT calculations were carried out with GAUSSIAN 98.<sup>17</sup>

## Materials

All solvents (Aldrich) are spectroscopic grade and were used as received. THF was refluxed over sodium and distilled under argon prior to use.

## 2-azido-3,5-dichlorobiphenyl

A solution of 2.2 g (13 mmol) of *ortho*-amino-biphenyl in 40 mL of  $\text{CCl}_4$  was stirred in an ice bath and continuously bubbled with chlorine gas. The reaction flask was connected to a chlorine gas trap. The white precipitate, which separated was collected after one hour, washed with  $\text{CCl}_4$ , and dried by exposure to the air. The crude product of 3.33 g was passed through a silica gel column with 10% ethyl acetate and 90% hexane to separate the dichlorinated compound (first component to run through the column) from the monochlorinated product to give 1.47 g (41% yield) of 3,5-dichloro-2-aminobiphenyl hydrochloride, as a white solid. GC/MS analysis found  $\text{M}^+$  at 237  $m/z$  and  $\text{M}^+$ : ( $\text{M} + 2$ )<sup>+: ( $\text{M} + 4$ )<sup>+</sup> was 9: 6: 1. To a solution of 1.47 g (5.4 mmol) of 3,5-dichloro-2-aminobiphenyl hydrochloride in 10 mL of THF was added a mixture of concentrated hydrochloric acid (2.5 mL) and water (20 mL). The reaction mixture was stirred for 15 min in an ice bath, and a solution of 700 mg (10 mmol) of  $\text{NaNO}_2$  in 10 mL was added drop-wise to the solution, keeping the temperature of the reaction mixture below 5 °C. The reaction mixture was stirred for 15 min at 0 °C, and excess nitrous acid was removed by the addition of urea. To the cooled reaction mixture was added drop-wise a solution of 900 mg (13.8 mmol) of  $\text{NaN}_3$  in 10 mL of water. After the addition was complete, the reaction mixture was stirred for 1.5 h at room temperature. The organic material was extracted with diethyl ether, and the extract was washed with dilute hydrochloric acid (0.1 M) and dried over anhydrous  $\text{Na}_2\text{SO}_4$ . The solvent was removed under reduced pressure, and the residue was developed on a silica gel column with *n*-pentane and was then recrystallized in methanol/pentane</sup>

under dry ice to give 470 mg (1.8 mmol, 33% yield) of 3,5-dichloro-2-biphenylazide as white crystals (needles). Mp 53.5–54.5 °C; IR (KBr) 2114  $\text{cm}^{-1}$  ( $\text{N}_3$ ); HRMS calcd. for  $\text{C}_{12}\text{H}_7\text{Cl}_2\text{N}_3$  263.00115, found 262.9994  $m/z$ .

## 2-azido-3,5-dichlorobiphenyl-d<sub>7</sub>

The synthesis of this compound follows the same procedure as that of 3,5-dichloro-2-biphenyl azide, except that *ortho*-aminobiphenyl-d<sub>9</sub> (CDN Isotopes, Inc.) was used as starting material and that the amount of starting reagent was reduced to one fifth the original quantity. 3,5-dichloro-2-biphenylazide-d<sub>7</sub> was obtained as white crystals (needles). Mp 53.5–54.5 °C; IR (KBr) 2123  $\text{cm}^{-1}$  ( $\text{N}_3$ ), 2286, 2358  $\text{cm}^{-1}$  (C–D); HRMS calcd. for  $\text{C}_{12}\text{D}_7\text{Cl}_2\text{N}_3$  270.0456, found 270.0558  $m/z$ . The base peak in the MS was  $\text{M} - \text{N}_2$ , as expected (observed 242.0368, calculated 242.0395  $m/z$ ).

## Results and discussion

### Laser flash photolysis of 2-azido-3,5-dichlorobiphenyl, nanosecond time scale

Laser flash photolysis (LFP, 266 nm, 5 ns) of 3,5-dichloro-2-biphenyl azide in glassy methylcyclohexane at 77 K produces the transient absorption spectra of Fig. 1. The transient spectrum, recorded immediately after the flash (spectrum 1), has  $\lambda_{\text{max}} = 435$  nm and decays with an observed rate constant of  $1.4 \pm 0.1 \times 10^7 \text{ s}^{-1}$  ( $\tau = 71 \pm 5$  ns). The decay of this species is accompanied by the growth ( $k_{\text{obs}} = 1.5 \pm 0.1 \times 10^7 \text{ s}^{-1}$ ) of absorption, centered at 355 nm, with a weaker absorption at 413 nm (spectrum 2). The latter spectrum is identified as that of triplet nitrene **3Tb**, which can be formed as a persistent species by continuous irradiation of **1b** at 77 K (spectrum 3). Thus, the singlet nitrene **3Sb** has been detected by LFP of **1b** at 77K ( $\lambda_{\text{max}} = 415, 435, 455$  nm) and it relaxes cleanly to the lower energy triplet (**3Tb**) under these conditions.

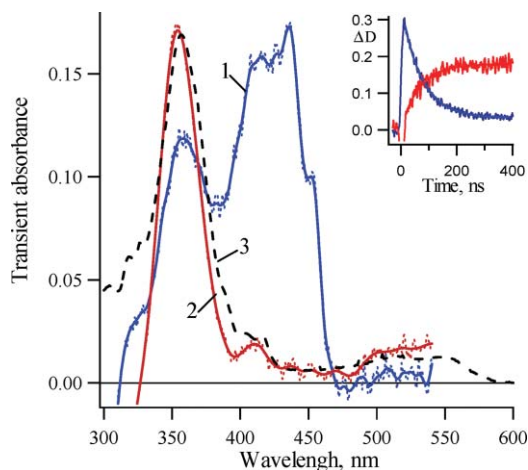


**Fig. 1** Transient absorption spectra detected over a window of 10 ns following LFP (266 nm, 5 ns) of 2-azido-3,5-dichlorobiphenyl (**1b**) in glassy methylcyclohexane (MCH) at 77 K (1) just after the laser pulse and (2) 200 ns after the laser pulse; (3) the persistent spectrum of triplet 3,5-dichloro-2-biphenylnitrene (**3Tb**) produced by brief photolysis (10 s, 254 nm) of **1b** in MCH at 77 K. Inset: Kinetic traces for decay of singlet 3,5-dichloro-2-biphenyl nitrene **3Sb** at 430 nm and growth of triplet nitrene **3Tb** at 355 nm.

The resulting transient spectra resemble those obtained upon LFP of 2-biphenyl azide (**1a**) at 77 K.<sup>1</sup> The chlorine substitution has little influence on the intersystem rate constant ( $k_{\text{ISC}} = k_{\text{obs}}$  at 77 K). Compared to the absorption maxima of unsubstituted *ortho*-biphenyl nitrene **3a**, the chlorine substituted compound exhibits a perceptible red shift. The magnitude of the red shift is about 15 nm in singlet nitrene **3S** and is about 10 nm in triplet nitrene **3T**.

At ambient temperature, LFP (266 nm, 5 ns) of 3,5-dichloro-2-biphenyl azide in pentane produces the transient absorption spectra of Fig. 2. A broad intense visible band ranging from 400 to 500 nm was observed 15 ns after the laser flash. This transient absorption decays exponentially at ambient temperature (Fig. 2, insert), and its disappearance proceeds with concurrent formation of the chlorinated carbazole **2b**. The first order rate constants obtained by the fitting of the decay and growth observed between 290–570 nm coincide (with an accuracy of  $\pm 20\%$ ). However, there is a tendency for the rate constants in the region of 400–440 nm to be smaller than those measured in the 450–550 nm region.

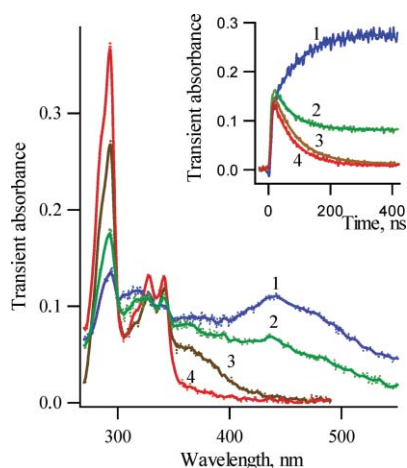


**Fig. 2** Transient absorption spectra detected over a window of 10 ns following LFP (266 nm, 5 ns) of 3,5-dichloro-2-biphenyl azide **1b** in pentane at ambient temperature (1) about 15 ns after the laser pulse and (2) 60 ns, (3) 1  $\mu$ s and (4) 30 ms after the laser pulse. Inset: Kinetic traces (1) for the growth of carbazole absorption at 294 nm and the decay of its precursors (2) at 320 nm, (3) 440 nm and (4) 470 nm.

Both the transient spectrum and the kinetics of the species absorbing in the visible region (Fig. 2) are very similar to those of the isocarbazole **6a** produced by LFP of 2-biphenyl azide (**1a**). It is worth mentioning that the transient absorption in visible region, obtained by LFP of **1b**, is much more intense than that of **1a**, presumably due to a lower rate constant of azirine-formation of **3Sb**, a process which competes with the formation of **6b**. Thus, whereas unsubstituted carbazole formation takes place mainly on the millisecond time scale at ambient temperature with didehydroazepine (**5a**) serving as a reservoir of the singlet 2-biphenyl nitrene (**3Sa**), the chlorinated carbazole **2b** is produced predominantly on the nanosecond time scale and only to a minor extent from the corresponding didehydroazepines **5b** and/or **5b'**.

As with the case of unsubstituted compound **1a**, LFP of **1b** in acetonitrile produces transient absorption spectra (Fig. 3), which are different from those, observed in pentane (Fig. 2). Intense absorption with a maximum at 440 nm and a shoulder at 470 nm, which is observed in pentane, is absent from the transient spectrum detected 15 ns after the laser pulse in acetonitrile. Nevertheless, a transient absorption with shoulders at 415 and 440 nm and a less intense band at 500–550 nm was detected in this solvent. Its decay, with rate constant  $2.1 \pm 0.1 \times 10^7 \text{ s}^{-1}$  ( $\tau = 48 \pm 3 \text{ ns}$ ), was accompanied by the growth of the substituted carbazole **2b** with the same rate constant (Fig. 3, insert A). This process was not observed in the case of **1a**.<sup>1</sup> The failure to observe this process in the parent system may be due to very small transient absorption of the non-chlorinated intermediate. It is also possible, that the corresponding intermediate and process does not exist in the unsubstituted system. At this time the carrier (**7b**) of this spectrum with  $\lambda_{\text{max}} = 415$  and 440 nm ( $\tau = 48 \pm 3 \text{ ns}$ ) is not assigned.

Additional growth of the carbazole absorption was detected on the microsecond time scale (Fig. 3, insert B). As with parent compound **1a**,<sup>1</sup> the corresponding didehydroazepines **5b** and/or

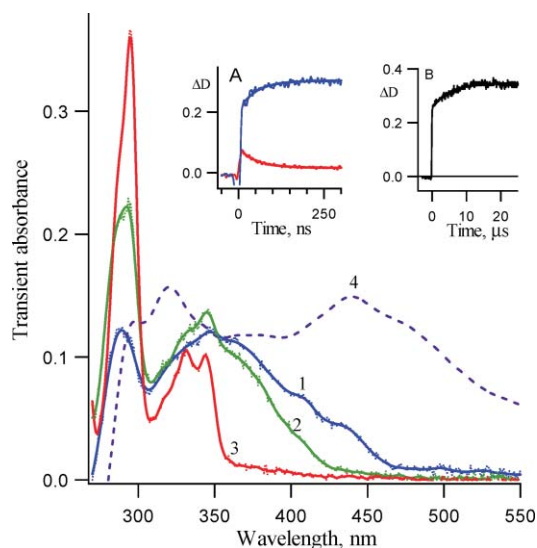
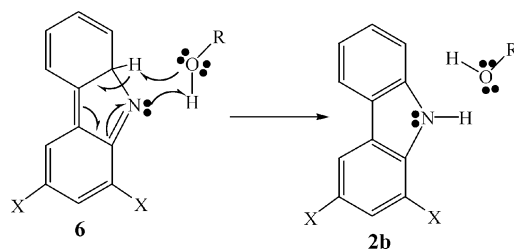


**Fig. 3** Transient absorption spectra detected over a window of 10 ns following LFP (266 nm, 5 ns) of 3,5-dichloro-2-azido biphenyl **1b** in acetonitrile at ambient temperature (1) about 15 ns, (2) 250 ns and (3) 300  $\mu$ s after the laser pulse. (4) For comparison, the transient absorption spectrum detected in pentane 15 ns after laser pulse is also presented. Inset: (A) Kinetic traces for growth of carbazole **2b** at 294 nm and decay of its precursor at 440 nm. (B) Growth of the carbazole absorption at 294 nm on a microsecond time scale.

**5b'** eventually isomerizes to carbazole **2b** on this time scale ( $\tau = 6 \pm 1 \mu$ s).

As in our previous study,<sup>1</sup> we propose that trace quantities of water in acetonitrile catalyze the transformation of **6b** into **2b**. A reasonable mechanism for this catalysis is shown in Scheme 3. Fig. 4A displays the acceleration of the decay, monitored at 470 nm, in dichloromethane in the presence of 'wet'  $\text{CH}_3\text{CN}$ . Curiously, the kinetic traces in the presence of  $\text{CH}_3\text{CN}$  are clearly biexponential, which indicates that two species absorb at this wavelength, but that only one of these intermediate reacts efficiently with water. The pseudo-first order rate constant of isocarbazole **6b** disappearance in 'wet' acetonitrile was estimated to be  $9 \pm 2 \times 10^8 \text{ s}^{-1}$ .



**Scheme 3**

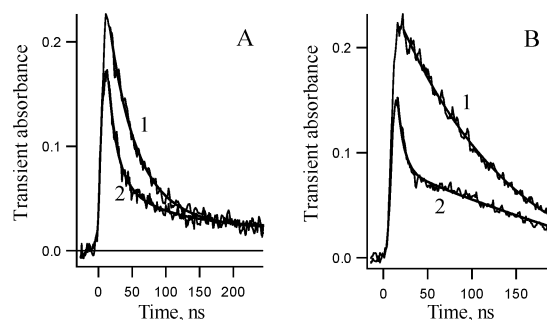


**Fig. 4** Kinetics of transient absorption decay at 470 nm at ambient temperature. (A) Kinetics detected in  $\text{CH}_2\text{Cl}_2$  in the absence (1) and in the presence (2) of 1.74 M of  $\text{CH}_3\text{CN}$  and (B) kinetics detected in pentane in the absence (1) and in the presence (2) of  $6.7 \times 10^{-3} \text{ mol l}^{-1}$  of 1-propanol.

Fig. 4B demonstrates that 1-propanol also accelerates the disappearance of **6b** very efficiently. The rate constant of the reaction of isocarbazole **6b** with 1-propanol is estimated to be diffusion controlled ( $k = 1.9 \pm 0.3 \times 10^{10} \text{ M}^{-1} \text{ s}^{-1}$ ). At the same time the influence of 1-propanol on the lifetime of the second intermediate (**7b**) absorbing at 440 nm is not pronounced and its lifetime was found to be  $53 \pm 3 \text{ ns}$  in neat 1-propanol. The transient spectrum detected in neat 1-propanol 15 ns after the laser pulse is very similar to the transient spectrum in  $\text{CH}_3\text{CN}$ , but is about twice as intense (Fig. 3).

Additional information on the kinetics and spectroscopy of the above-mentioned intermediates can be obtained *via* low temperature experiments. LFP (266 nm, 5 ns) of **1b** in pentane at 161 K produces the transient absorption spectra of Fig. 5. A very intense transient absorption was observed in the visible region. The visible absorption band detected 55 ns after the laser pulse is similar to the absorption band detected at ambient temperature (Fig. 2, spectrum 1), but shows a structured shape. However, after a few hundreds of nanoseconds, it is replaced by a broad unstructured band (Fig. 5, spectrum 3), which disappears within several microseconds. Thus, after three hundred nanoseconds, the spectrum of the unassigned intermediate **7b** ( $\lambda_{\text{max}} = 425$ , 440 nm) disappears, and only the broad unstructured band of **6b** ( $\lambda_{\text{max}} = 470 \text{ nm}$ , spectrum 3) is observed. Note, that dichlorinated isocarbazole **6b** also has an intense absorption band with a maximum at about 320 nm, similar to the case of unsubstituted compound **6a**.<sup>1</sup>

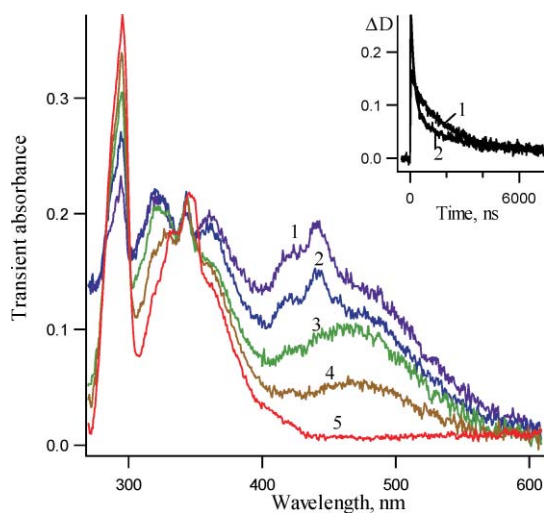
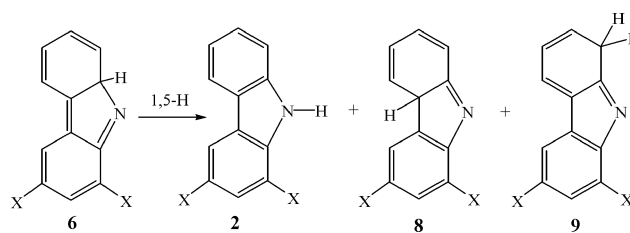


**Fig. 5** Transient absorption spectra detected over a window of 10 ns following LFP (266 nm, 5 ns) of 3,5-dichloro-2-azido biphenyl **1b** in pentane at 161 K (1) 55 ns, (2) 100 ns, (3) 300 ns, (4) 1.3  $\mu\text{s}$  and (5) 6  $\mu\text{s}$  after the laser pulse. Insert: kinetic traces for the absorption decay at (1) 475 nm and (2) 440 nm. The best fit for the trace (1) is exponential with  $k_{\text{obs1}} = 5.1 \pm 0.1 \times 10^5 \text{ s}^{-1}$ . The best bi-exponential fit for trace (2) gives  $k_{\text{obs1}} = 4.8 \pm 0.3 \times 10^5 \text{ s}^{-1}$  and  $k_{\text{obs2}} = 5.3 \pm 0.2 \times 10^6 \text{ s}^{-1}$ .

The lifetimes of the two intermediates (**6b** and **7b**) differ significantly (by about one order of magnitude) at 161 K, which is opposite to the case at room temperature, where they are very similar. A kinetic curve recorded at 470 nm is exponential, while a kinetic curve obtained at 440 nm is clearly bi-exponential (Fig. 6, Insert). Therefore, this data provide additional strong support for the presence of two intermediates absorbing in the visible region.

Interesting results were obtained using a XeCl excimer laser (308 nm, 15 ns) as the excitation source. Fig. 6 presents a collection of transient absorption spectra recorded using different excitation sources (A and B) in pentane as well as in different solvents (C). The simplest way to assign these transient spectra is to propose as before, that two intermediates absorbing in the range 400–600 nm are formed upon photolysis of **1b**. One of these species is isocarbazole **6b**, which is the main

product, upon 266 nm excitation (Fig. 6A). In acetonitrile **6b** isomerizes to **2b** faster than the time resolution ( $\approx 5 \text{ ns}$ ) of the experiment, and only the second intermediate **7b** is detected in this solvent (Fig. 5C). This unassigned intermediate **7b** is formed in greater amounts, upon 308 nm excitation, presumably at the expense of isocarbazole **6b** (Fig. 6B). Upon comparing the transient spectra recorded about 400 ns after excitation with different laser sources, it is clear that similar amounts of carbazole **2b** are formed in every case, but that about twice the yield of the intermediate with  $\lambda_{\text{max}}$  around 360 nm is formed with longer wavelength excitation. Previously<sup>1</sup> it was shown for parent compound **1a**, that two intermediates, azepine (**5a'**) and an isocarbazole **8a** (formed by the 'wrong' 1,5-hydrogen shift in **6a**, Scheme 4), have absorption bands, with maxima around 360 nm. The carriers of 360 nm transient absorption produced upon LFP of **1b** are likely analogous dichlorinated azepines and isocarbazoles.



**Scheme 4**

The temperature dependence of the rate constants for the disappearance of both intermediates was studied and the data are presented in Fig. 7. We measured the rate constant for the disappearance of isocarbazole **6b** ( $k_{\text{obs1}}$ ) in pentane at 470 nm using the YAG laser (266 nm, 5 ns) as an excitation source. The second rate constant ( $k_{\text{obs2}}$ ) was estimated using mainly the excimer laser excitation (308 nm, 15 ns). The kinetics were measured at either 400 or 440 nm for the unassigned species **7b**.

The magnitude of  $k_{\text{obs1}}$  decreases with temperature until approximately 170 K whereupon a limiting value ( $k_{\text{infl}}$ ) is reached (Fig. 7A, curve 1) in a manner reminiscent of 8aH-carbazole (**6a**). We previously assigned this type of temperature dependence for **6a** to a change in mechanism.<sup>1</sup> For example, a 1,5-hydrogen shift at higher temperature might be replaced by a catalyzed process at low temperature, which has a lower enthalpy of activation and a more negative entropy of activation. Alternatively, a contribution of quantum mechanical tunneling to the 1,5-hydrogen shift reaction that forms **2b** from **6b** could be responsible for the data obtained at low temperature. The Arrhenius treatment of  $\ln k_{\text{obs1}}$  versus  $1/T$  is curved while a straight line is obtained by plotting  $\ln(k_{\text{obs1}} - k_{\text{infl}})$  (Fig. 7B). The activation energy  $E_{\text{a1}} = 3.9 \pm 0.2 \text{ kcal mol}^{-1}$  is obtained from a plot of Fig. 7B and is similar to the value obtained with parent isocarbazole **6a**.<sup>1</sup> The pre-exponential factor was found to be  $A = 10^{9.7 \pm 0.1} \text{ s}^{-1}$ .

It is seen from Fig. 7A that the decay rate constant for the second intermediate **7b** changes slightly with temperature, by a factor of about 2.5 over the temperature range 150–290 K. Unfortunately, the accuracy of these data is very poor because the transient absorption of this intermediate and **6b** overlap significantly.

It must be noted that the temperature dependencies in Fig. 7A are very similar to those for the disappearance of singlet phenylnitrene and many of its derivatives.<sup>5</sup> In addition, the structured band of the intermediate **7b** with maxima at 415 and 435 nm is very similar to the absorption band of singlet nitrene **3Sb** (Fig. 6C). However, assignment of the transient absorbance at 415 and 435 nm to singlet nitrene **3Sb** can be excluded based on the rate of disappearance of this species observed at low temperatures. For singlet arylnitrenes the temperature dependence of the rate constant of disappearance

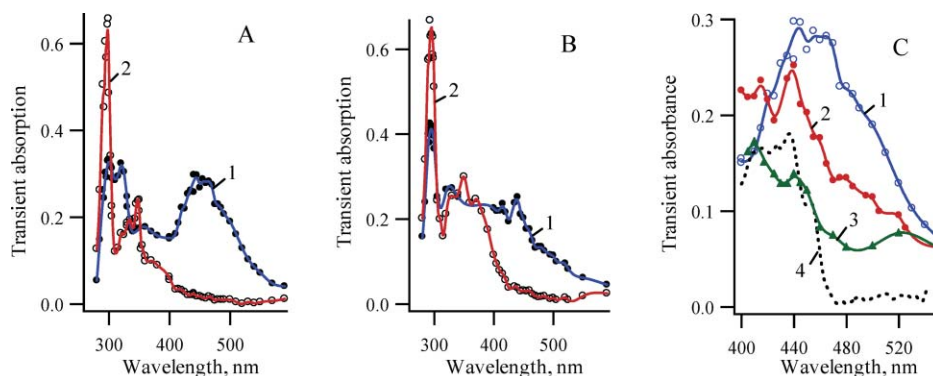


**Fig. 6** Transient absorption spectra detected following LFP of 2-azido-3,5-dichlorobiphenyl (**1b**) at ambient temperature, (A) in pentane using YAG laser (266 nm, 5 ns) (1) 20 ns and (2) 400 ns after the laser pulse; (B) in pentane using XeCl excimer laser (308 nm, 17 ns) (1) 35 and (2) 380 ns after the laser pulse; (C) The transient absorption spectra recorded tens of nanosecond after the laser pulse using different excitation sources and in different solvents: (1) in pentane (266 nm excitation), (2) in pentane (308 nm excitation) and (3) in acetonitrile (266 nm excitation). (4) Black line spectrum of singlet nitrene **3Sb** detected at 77 K.

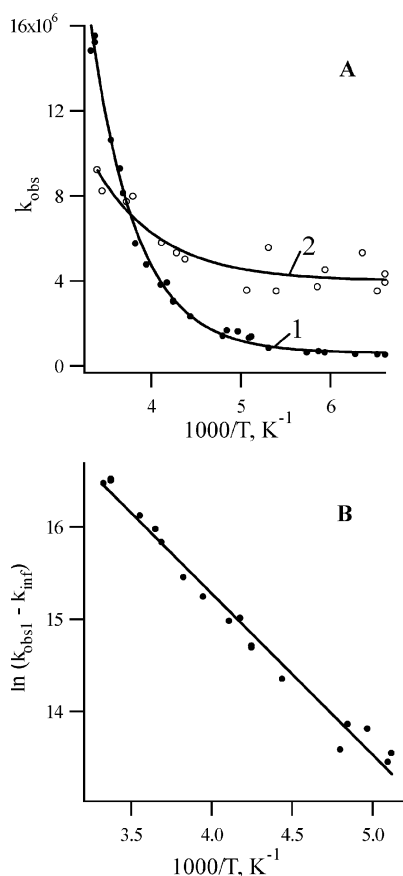


**Fig. 7** (A) The temperature dependence of the observed rate constants in pentane. (1)  $k_{\text{obs}1}$  of the isocarbazole **6b** decay measured at 470 nm following excitation by the YAG laser (266 nm, 5 ns). (2)  $k_{\text{obs}2}$  of the intermediate **7b** decay detected following excitation by the excimer laser (308 nm, 15 ns). (B) Arrhenius treatment of  $\ln(k_{\text{obs}1} - k_{\text{inf}})$  for the decay of **6b**.

can be described by eqn. (1) with the temperature-independent rate constant being that for intersystem crossing ( $k_{\text{ISC}}$ ).<sup>5</sup>

$$k_{\text{obs}} = k_{\text{R}} + k_{\text{ISC}} \quad (1)$$

If the temperature dependence of the rate constant for disappearance of the species **7b** is analyzed using eqn. (1), a value of  $k_{\text{ISC}} = (4 \pm 1) \times 10^6 \text{ s}^{-1}$  is obtained. However, the rate constant for intersystem crossing in **3Sb** measured at 77 K, was found to be much faster,  $(1.4 \pm 0.1) \times 10^7 \text{ s}^{-1}$ . It was shown recently for phenylnitrene (**1c**),<sup>18</sup> that  $k_{\text{ISC}}$  estimated from the low temperature data in liquid pentane is the same as measured at 77 K in MCH. This argues against assigning **7b** to singlet nitrene **3Sb**.

This conclusion will be confirmed by picosecond spectroscopy in a later section. These studies demonstrate that **3Sb** has  $\tau = 260 \pm 70 \text{ ps}$  in cyclohexane at ambient temperature. This lifetime is about 400 times shorter than the lifetime of the unassigned transient **7b** under comparable conditions.

The perdeuterated analogue of **1b** (**1b-d7**) was synthesized and studied by LFP techniques. As for the undeuterated compound, the spectra and kinetics obtained from **1b-d7** depend on the excitation source and solvent. It was shown above, that isocarbazole **6b** (with maxima at 320 and 470 nm) is formed mainly upon excitation of **1b** with a YAG laser (266 nm) in pentane. On the contrary, only a small amount of **6b** is formed upon excitation by 308 nm. The isocarbazole **6b** was not detected at all in acetonitrile and 1-propanol.

Therefore, to study the dependence of the lifetime of isocarbazole **6b** on deuteration, the kinetics at 320 and 470 nm was followed using the YAG laser source. The rate constant of transformation of **6b** to **2b** was measured at 295 K and found to be  $1.53 \pm 0.07 \times 10^7 \text{ s}^{-1}$  ( $\tau = 65 \pm 4 \text{ ns}$ ) and  $0.38 \pm 0.02 \times 10^7 \text{ s}^{-1}$  ( $\tau = 263 \pm 15 \text{ ns}$ ) for its perdeuterated analogue. The kinetic isotope effect (KIE) is deduced as  $k_{\text{H}}/k_{\text{D}} \approx 4.0 \pm 0.4$ , similar to that of unsubstituted **6a**.<sup>1</sup> If we deduce the effective KIE using kinetic data at 440 nm, the value drops to  $3.0 \pm 0.3$  due to the overlap of the spectra of two intermediates. The effective KIE estimated from kinetics monitored at 294 nm was found to be  $2.6 \pm 0.3$  and it confirms the existence of two channels of carbazole formation and that the KIE for the second reaction is smaller than that of **6b**.

If the excimer laser (308 nm) is used as the excitation source, a greater yield of the unassigned intermediate **7b** is observed and the apparent KIE determined at 440 nm drops to  $1.4 \pm 0.1$ , demonstrating that the KIE for the second reaction of carbazole formation is close to unity. Indeed, the KIE measured in acetonitrile and 1-propanol, where only intermediate **7b** absorbs in the visible region, is equal to  $0.95 \pm 0.10$ .

LFP of 2-azido biphenyl **1a** in fluid solution does not produce singlet nitrene **3Sa** as a detectable species on the nanosecond time scale. Only products of its transformation, azirine **4a** and isocarbazole **6a**, were detected as transient intermediates in solution.<sup>1</sup> Similarly we were unable to detect the dichlorinated singlet nitrene **3Sb** in fluid solution using nanosecond LFP. Only at very low temperature (below 170 K), were we able to detect very fast decay at 440 nm (the maximum of the **3Sb** absorption band, Fig. 1) and growth kinetics at 470 nm (the maximum of **6b** absorption band, Fig. 5) with the same rate constant (Fig. 8). The rate constant of the decay and growth at 147 K is measured to be  $5.5 \pm 0.7 \times 10^7 \text{ s}^{-1}$  ( $\tau = 18 \pm 3 \text{ ns}$ ). Therefore, to accurately determine the kinetics of singlet nitrene **3Sb** at room temperature, we used picosecond pump-probe techniques.

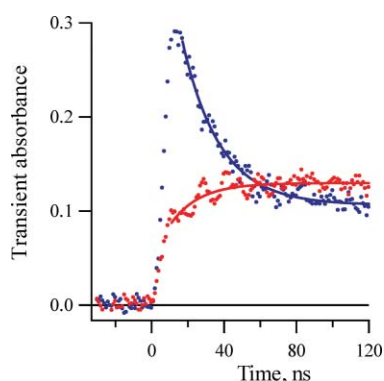


**Fig. 8** Kinetic traces of the growth of isocarbazole **6b** absorption at 470 nm and decay of its precursors **3Sb** at 440 nm detected after excitation (266 nm, 5 ns) of **1b** at 147 K in pentane.

### Picosecond pump-probe experiments

The transient absorption spectra shown in Fig. 9 were recorded in pump-probe experiments. The sample solution of **1b** in cyclohexane was pumped by a femtosecond laser pulse (220 fs, 265 nm) and the transient absorption spectra were recorded at different time delays between probe and pump pulses.

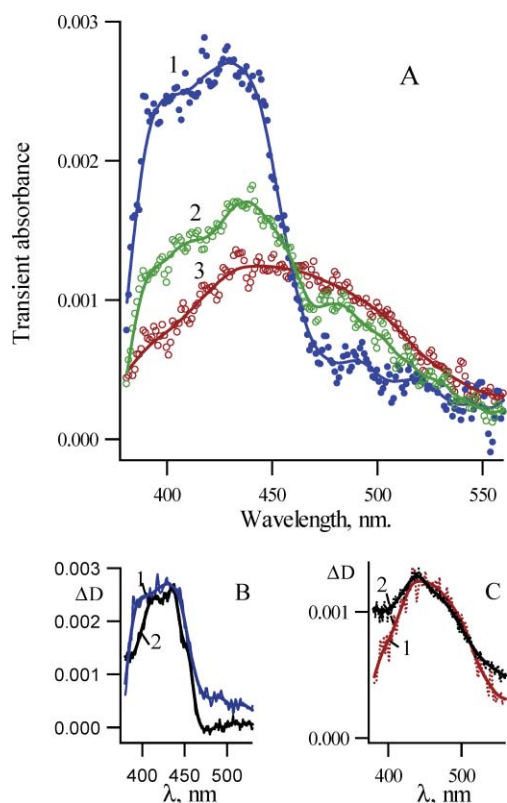


**Fig. 9** (A) Transient absorption spectra recorded in pump-probe experiments (265 nm, 220 fs) upon photolysis of 3,5-dichloro-2-azido-biphenyl **1b** in cyclohexane at ambient temperature (1) 40 ps, (2) 300 ps and (3) 630 ps after excitation. (B) Spectrum 1 is the same as in A1; (2) is the spectrum of singlet 3,5-dichloro-2-biphenylnitrene (**3Sb**) in MCH at 77 K detected by nanosecond LFP. (C) Spectrum 1 is the same as A3; spectrum 2 was detected over a window of 10 ns following LFP (266 nm, 5 ns) of 3,5-dichloro-2-azido biphenyl **1b** in pentane at ambient temperature about 15 ns after the laser pulse.

Fig. 9A shows, that the initially observed transient absorption with a maximum around 430 nm and a shoulder around 400 nm decays in hundreds of picoseconds to produce a new species with a broad absorption spectrum with a maximum around 440 nm. It is seen from Fig. 9B, that the spectrum recorded 40 ps after the excitation is very similar to the spectrum of the singlet nitrene detected at 77 K by nanosecond LFP. However, the spectrum

detected at 77 K has more pronounced structural features, which is typical for spectra recorded at cryogenic matrices. Therefore, we assign this spectrum with maximum at 430 nm to singlet 3,5-dichloro-2-biphenylnitrene **3Sb**. The final spectrum 3 is very similar to the spectrum detected around 15 ns after the laser pulse (Fig. 9C).

Additional details can be obtained from the kinetics of the transient absorption, which are shown in Fig. 10. Fig. 10 reveals, that the decay of singlet nitrene **3Sb** at 420 nm is accompanied by a growth in transient absorption with the same time constant at 470 nm, which was assigned to the isocarbazole **6b**. Exponential fit of these traces yields the rate constant of singlet nitrene rearrangement  $k_R = 3.8 \pm 0.8 \times 10^9 \text{ s}^{-1}$  ( $\tau = 260 \pm 70 \text{ ps}$ ).

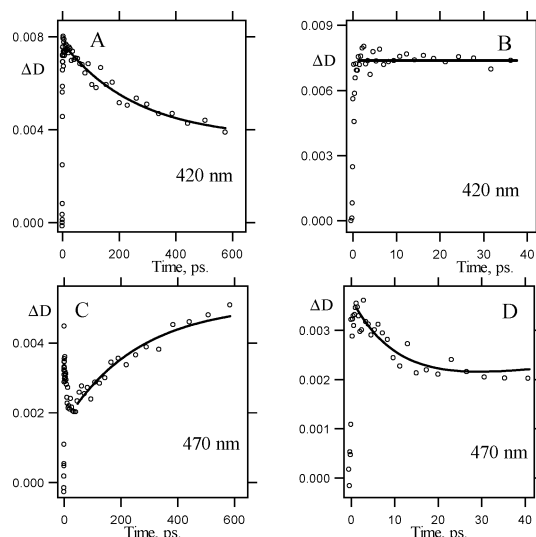


**Fig. 10** Transient absorption kinetics detected in pump-probe experiments (265 nm, 220 fs) upon excitation of 3,5-dichloro-*o*-biphenyl azide (**1b**) in cyclohexane at ambient temperature. Kinetics were recorded at 420 nm (A, B) and 470 nm (C, D) on different time scales: 0–633 ps (A, C) and 0–40 ps (B, D).

Therefore, we have monitored singlet nitrene **3Sb** decay in three different types of experiments. The rate constant of **3Sb** decay at room temperature ( $k_R = 3.8 \pm 0.8 \times 10^9 \text{ s}^{-1}$ ) was measured using the picosecond pump-probe technique. The rate constant over the temperature range 147–167 K was obtained using nanosecond LFP, and eventually, the rate constant of ISC was measured at 77 K. As before, we propose, that the temperature dependence of the rate constant of the singlet nitrene decay can be described by eqn. (1) with a temperature-independent intersystem crossing rate constant ( $k_{ISC}$ ).<sup>5</sup> Thus, we were able to calculate the Arrhenius parameters for the rate constant of singlet nitrene **3Sb** rearrangement (Fig. 11). The activation energy was found to be  $2.7 \pm 0.2 \text{ kcal mol}^{-1}$  with a pre-exponential factor  $A = 10^{11.6 \pm 0.2} \text{ s}^{-1}$ . The value of the activation energy is consistent with our recent calculations<sup>1</sup>

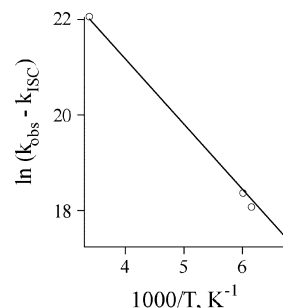


**Fig. 11** Arrhenius treatment of the decay rate constant of the singlet nitrene **3Sb** in pentane.

for **3Sa** cyclization to isocarbazole **6a** and computational data presented in the next section.

The kinetic curve recorded at room temperature at 420 nm on the time scale of few picoseconds demonstrates that singlet nitrene **3Sb** is formed faster than the time resolution of our apparatus (about 220 fs). Therefore we can conclude, that dissociation of the N–N bond in the excited state of the azide **1b** occurs with a rate constant  $k_{\text{dis}} \geq 5 \times 10^{12} \text{ s}^{-1}$ .

However, we were able to detect a fast decay of transient absorption at longer wavelengths. A kinetic curve recorded at 470 nm is displayed in Fig. 10 as an example. The time constant for this decay was estimated to be  $0.9 \pm 0.2 \times 10^{11} \text{ s}^{-1}$  ( $\tau = 11 \pm 2 \text{ ps}$ ). This time constant is typical of a vibrational relaxation process, which manifests itself in a narrowing of the absorption band.<sup>19</sup>

The spectrum detected 40 ps after the pump laser pulse also has a shoulder at about 480 nm (Fig. 9, spectrum 1), which apparently is not due to the singlet nitrene. Presumably, the carrier of this transient absorption is one of the species detected on the nanosecond time scale (Fig. 9, spectrum 3). We speculate, that the carrier of transient absorption detected in the region 460–550 nm 40 ps after the pump pulse is the isocarbazole **6b**, formed from a vibrationally hot state of the singlet nitrene **3Sb**\*

A very similar transient absorption spectrum with a strong absorption band around 420 nm was observed in methanol 15 ps after excitation of **1b** (Fig. 12, spectrum 1) and is also assigned to the singlet nitrene **3Sb**. A considerable acceleration of the singlet nitrene rearrangement (presumably to **6b** and **7b**) was observed in methanol. The rate constant of its decay was found to be  $1.6 \pm 0.2 \times 10^{10} \text{ s}^{-1}$  ( $62 \pm 10 \text{ ps}$ ). A similar acceleration of the singlet tolylnitrene rearrangement in alcohols has been observed.<sup>20</sup> The transient spectrum detected 500 ps after the laser pulse is similar to the spectrum detected in acetonitrile and 1-propanol. Therefore, isocarbazole **6b**, which should be formed due to rearrangement of **3Sb**, will react very rapidly with methanol to form carbazole **2b**. We believe this assumption is reasonable, after taking into account the diffusion-controlled nature of this reaction.

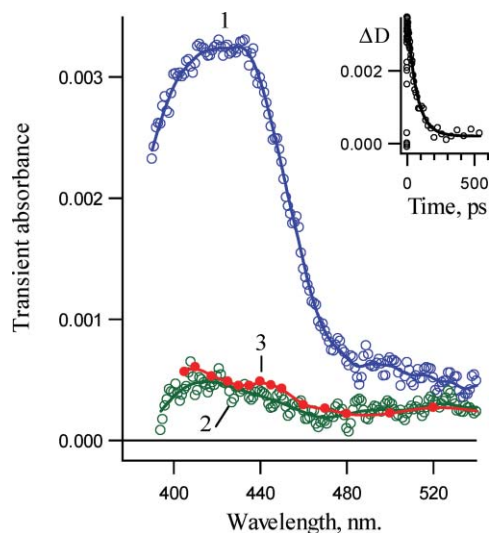


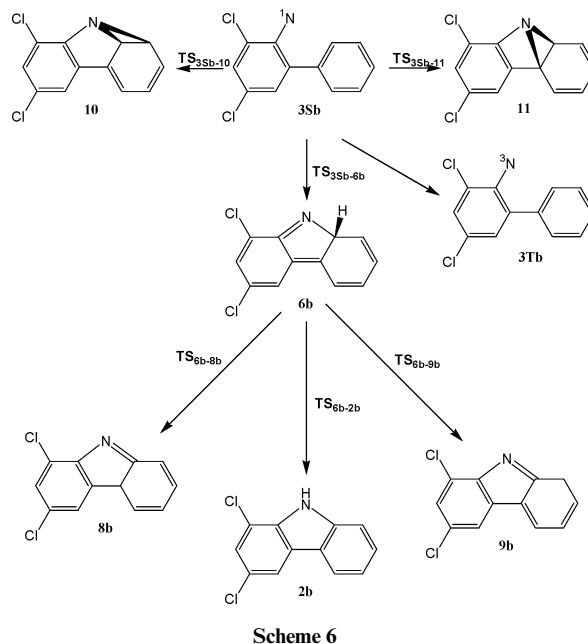
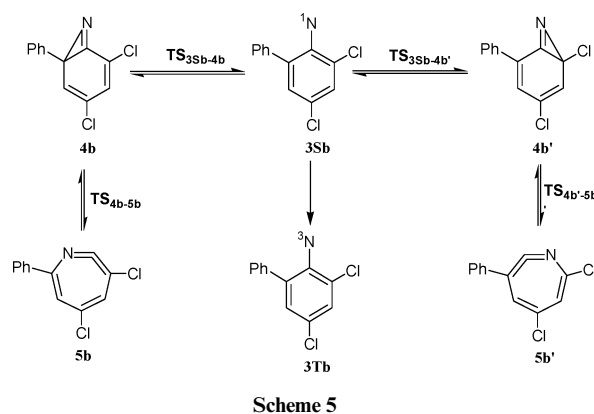
**Fig. 12** Transient absorption spectra detected in pump–probe experiments (265 nm, 220 fs) upon excitation of 3,5-dichloro-2-azido-biphenyl (**1b**) in methanol at ambient temperature: (1) 15 ps and (2) 500 ps after pump pulse. Curve 3 is the spectrum detected 20 ns after the laser pulse (266 nm, 5 ns) in acetonitrile recorded by convention LFP. Insert: Kinetics detected at 420 nm.

### Calculations of 3,5-dichloro-2-biphenylnitrene and related species

Recently,<sup>1</sup> the stationary points on the potential energy surface of singlet 2-biphenylnitrene (**3Sa**) and its ring-expansion and

intramolecular cyclization reactions to isocarbazole **6a** were computed using the high level (14,14)CASSCF/CASPT2 procedure, in addition to more simple estimations based on the B3LYP calculations. In this work, only the latter more simple estimations were performed for the dichlorosubstituted nitrene **3Sb** and its reaction.

First, the absolute CASPT2(8,8)/6-31G\* energies for the CASSCF(8,8)/6-31G\* optimized geometries of singlet nitrene **3Sb** and triplet nitrene **3Tb** were determined to be  $-1433.750077$  and  $-1433.778136 E_h$ , respectively. Thus, the singlet–triplet energy gap ( $\Delta E_{\text{ST}}$ ) of **3Sb/3Tb** is predicted to be  $17.6 \text{ kcal mol}^{-1}$ , which is very close to that of unsubstituted biphenylnitrene **3a** and parent phenylnitrene **3c**.<sup>1,10</sup> Secondly the DFT energies of the stationary points involved in the ring-expansion reactions (Scheme 5) and intramolecular cyclization reactions (Scheme 6) of **3Sb** (except for that of **3Sb** itself) were performed using B3LYP/6-31G\* geometry optimizations, zero-point energy calculations, and single point energy calculations using B3LYP/6-311+G(2,d,p) methods. These calculated energies are given in Tables 1 and 2, respectively. Finally, the relative energies of all stationary points corresponding to **3Sb** are deduced from the DFT energies and CASPT2  $\Delta E_{\text{ST}}$  by using triplet nitrene **3Tb** as a common basis.



These relative energies are listed in Tables 1 and 2 as well, and the calculated potential energy surfaces for the ring-expansion and intramolecular cyclization reactions of **1b** are depicted in Fig. 13 and 14, respectively.

Inspection of the data in Table 1 and Fig. 13 reveals that chlorine substitution does raise the barrier to ring-expansion of

**Table 1** Calculated absolute energies ( $E_h$ ), ZPE, and DFT/CASPT2 relative energies ( $\text{kcal mol}^{-1}$ ) for stationary species involved in the ring-expansion reactions of singlet 3,5-dichloro-2-biphenylnitrene **3Sb**

Species	B3LYP/6-31G*	ZPE <sup>a</sup>	B3LYP/6-311+G(2d,p)	Relative energy <sup>b</sup>
<b>3Tb</b>	-1436.551411	96.21	-1436.751619	-17.6
<b>TS<sub>3Sb-4b'</sub></b>	-1436.505894	95.51	-1436.708620	8.7
<b>4b'</b>	-1436.530208	96.65	-1436.730184	-3.7
<b>TS<sub>4b'-5b'</sub></b>	-1436.519476	95.60	-1436.720341	1.4
<b>5b'</b>	-1436.536804	96.62	-1436.740096	-10.0
<b>TS<sub>3Sb-4b</sub></b>	-1436.506421	95.61	-1436.708907	8.6
<b>4b</b>	-1436.520764	96.46	-1436.721656	1.4
<b>TS<sub>4b-5b</sub></b>	-1436.514554	95.67	-1436.715655	4.4
<b>5b</b>	-1436.533471	96.81	-1436.736250	-7.4

<sup>a</sup> B3LYP/6-31G\* zero point vibrational energies. <sup>b</sup> (U)B3LYP/6-311+G(2d,p)/(U)B3LYP/6-31G\* + ZPE relative energies to **3Sb** combined with CASPT2  $\Delta E_{ST}$ .

**Table 2** Calculated absolute energies ( $E_h$ ), ZPE, and DFT/CASPT2 relative energies ( $\text{kcal mol}^{-1}$ ) for stationary species involved in the intramolecular cyclization reactions of singlet 3,5-dichloro-2-biphenylnitrene **3Sb**

Species	B3LYP/6-31G*	ZPE <sup>a</sup>	B3LYP/6-311+G(2d,p)	Relative energy <sup>b</sup>
<b>3Tb</b>	-1436.551411	96.21	-1436.751619	-17.6
<b>TS<sub>3Sb-6</sub></b> <sup>c</sup>	-1436.520573	95.66	-1436.721421	0.8
<b>6b</b>	-1436.571772	97.47	-1436.772699	-29.6
<b>TS<sub>3Sb-11b</sub></b> <sup>c</sup>	-1436.501351	96.12	-1436.701589	13.7
<b>11b</b>	-1436.511404	97.21	-1436.710426	9.2
<b>TS<sub>3S-10b</sub></b> <sup>c</sup>	-1436.490029	96.16	-1436.689676	21.2
<b>10b</b>	-1436.495407	97.59	-1436.693861	20.0
<b>TS<sub>6b-2b</sub></b>	-1436.556187	95.58	-1436.758405	-22.5
<b>2b</b>	-1436.661711	98.98	-1436.863362	-85.0
<b>TS<sub>6b-9b</sub></b>	-1436.552369	95.49	-1436.754227	-20.0
<b>9b</b>	-1436.611798	98.00	-1436.810754	-52.9
<b>TS<sub>6b-8b</sub></b>	-1436.553003	95.60	-1436.755212	-20.5
<b>8b</b>	-1436.598348	97.91	-1436.799081	-45.7

<sup>a</sup> B3LYP/6-31G\* zero point vibrational energies. <sup>b</sup> DFT/CASPT2 relative energies, derived from the B3LYP/6-311+G(2d,p)/B3LYP/6-31G\*+ZPE energies relative to **3Tb** minus the CASPT2  $\Delta E_{ST}$  of **3Sb/3Tb**. <sup>c</sup> Broken symmetry B3LYP calculations (UB3LYP) were applied.

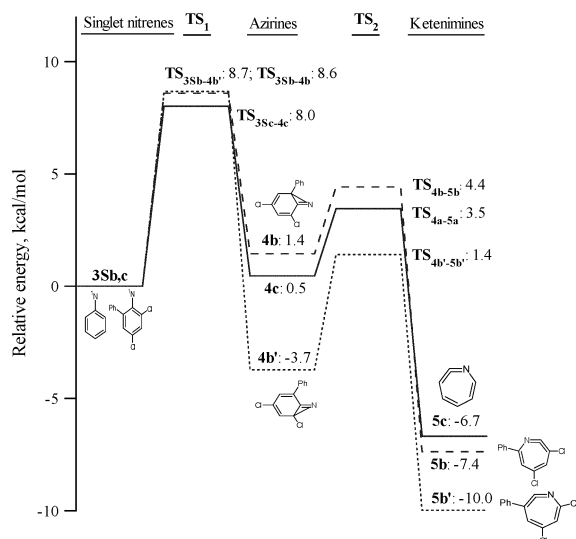


**Fig. 13** DFT/CASPT2 energies relative to singlet nitrenes for the species involved in the ring-expansion reactions of singlet 3,5-dichloro-2-nitrenebiphenyl **3Sb** and phenylnitrene (**3Sc**).

**3Sb** relative to singlet phenylnitrene. As depicted in Fig. 13, the barrier to ring-expansion by cyclization toward either the *ortho*-chlorine substituted carbon or the *ortho*-phenyl substituted carbon (Scheme 5) are similar and about  $1 \text{ kcal mol}^{-1}$  higher than that of unsubstituted phenylnitrene. In comparison with the barrier to ring-expansion of unsubstituted *ortho*-biphenylnitrene **3Sa**, chlorine substitution raises the barrier to ring-expansion of **3Sb** by  $3.8 \text{ kcal mol}^{-1}$ .

Note, that theory predicts that the rate-determining step in the two-step ring-expansion reaction sequence of **3Sb** is the first step,

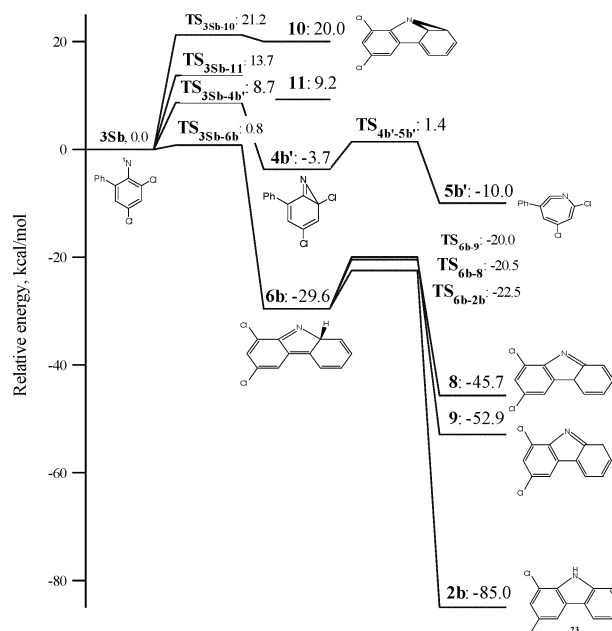


**Fig. 14** DFT/CASPT2 energies relative to the singlet 3,5-dichloro-2-biphenylnitrene **3Sb** for species involved in the intramolecular cyclization and ring-expansion reactions.

the formation of an azirine. The opposite situation was observed in unsubstituted *o*-biphenylnitrene **3Sa**, for which the second step is the rate determining reaction.<sup>1</sup> Therefore unsubstituted azirine **4a** was detected as transient intermediate over the entire temperature range studied ( $150\text{--}298 \text{ K}$ ).



Examination of the data in Table 2 and Fig. 14 reveals that the calculated potential energy surfaces for several intramolecular cyclization reactions of **3Sb** are very similar to those of singlet *ortho*-biphenyl nitrene.<sup>1</sup> The results demonstrate that chlorine substitution does not distinctly influence any of the intramolecular cyclization reactions of singlet *ortho*-biphenylnitrene other than azirine formation. Thus, **3Sb** should cyclize effectively to dichloroisocarbazole **6b**, and with an elementary rate constant analogous to the parent 2-biphenyl nitrene system.

More sophisticated (14,14)CASSCF/CASPT2 calculations, which were done for the parent nitrene **3Sa**, predicted the barrier for the cyclization to isocarbazole **6a** to be 6 kcal mol<sup>-1</sup>. Taking into account the fact, that this procedure usually overestimates the barrier for the cyclization of singlet arylnitrenes by about 3 kcal mol<sup>-1</sup>,<sup>5b,c,3,9</sup> we can estimate barrier for cyclization of **3Sa** to **6a** (as well as **3Sb** to **6b**) to be about 3 kcal mol<sup>-1</sup>. This value is in perfect agreement with experimentally estimated activation energy for the rearrangement of the singlet nitrene **3Sb**.

Previously,<sup>1</sup> the electronic absorption spectra of the intermediates (**4a'**, **5a'**, **6a** and **8a–11a**), proposed for the rearrangement of unsubstituted 2-biphenyl azide, were calculated using time-dependent (TD) DFT theory with the random phase approximation.<sup>10</sup> The data of these calculations were used to support the assignment of the transient spectra.<sup>1</sup> It is clear that chlorine substituents do not significantly change the spectra of these intermediates and the data obtained in previous calculations can model the intermediates of photolysis of **1b**.

The unidentified intermediate **7b** has an absorption with  $\lambda_{\max}$  = 415, 435 and 530 nm. Among all the proposed intermediates (Schemes 5 and 6), which can be formed due to the **3Sb** cyclization reactions only **10b** and azepine **5b**, produced *via* cyclization toward the phenyl ring, have absorption bands in the visible region. The spectrum of **10a** was found to have the following absorption bands ( $\lambda_{\max}$  and oscillator strength): 462 (0.007), 322 (0.031) and 275 (0.097).<sup>1</sup> The spectrum of didehydroazepine **5b** was found to have  $\lambda_{\max}$  432 nm (0.023), 390 nm (0.017) and 304 nm (0.259). However, according to the calculations the formation of these intermediates is unfavorable due to the very high barriers for these rearrangements (Fig. 13, Table 1).

It was noted before, that the absorption spectrum of **7b** (415, 435 nm) resembles the spectrum of **3Sb** and the temperature dependence of its kinetics is typical of singlet arylnitrenes. Therefore, at this time the only tentative assignment of this intermediate (**7b**) is to a complex between the nitrene and the pendant phenyl ring. More calculations and experiments must be performed to support or exclude this assignment.

## Conclusions

Laser flash photolysis (LFP) of 3,5-dichloro 2-biphenyl azide releases the corresponding singlet nitrene **3Sb**. At 77 K, nitrene **3Sb** (415, 435, 455 nm) has a lifetime of 71 ± 3 ns controlled by intersystem crossing to the lower energy triplet state (**3Tb**;  $\lambda_{\max}$  = 355 nm). CASPT2 (8,8) 6-31G\* calculations predict that triplet nitrene **3Tb** is 17.6 kcal mol<sup>-1</sup> lower in energy than singlet nitrene **3Sb**, an amount similar to that of parent singlet phenylnitrene. LFP of 3,5-dichloro-2-biphenyl azide at ambient temperature releases singlet nitrene **3Sb**, which rearranges to isocarbazole **6b** ( $\lambda_{\max}$  = 470 nm) and unidentified intermediate **7b** with  $\lambda_{\max}$  = 415, 435 and 530 nm. The lifetime of **3Sb** at room temperature was found to be 260 ± 70 ps in cyclohexane and 62 ± 70 ps in methanol. The activation energy of the **3Sb** rearrangement (2.7 ± 0.2 kcal mol<sup>-1</sup>) is in excellent agreement with the computed barrier for cyclization to isocarbazole.

The lifetime of isocarbazole **6b** is 65 ± 4 ns in pentane at ambient temperature. The lifetime of **6b–d7** is 263 ± 15 ns under the same conditions corresponding to a KIE of 4.0 ± 0.4. This value is very reasonable for the dichlorinated isocarbazole isomerization to the corresponding carbazole by 1,5-hydrogen

shift. The rearrangement reaction is both alcohol and water catalyzed.

The unidentified intermediate **7b** with  $\lambda_{\max}$  = 415, 435 and 530 nm also rearranges to the dichlorinated carbazole **2b**. The rate of its rearrangement in pentane at 295 K is about 1.5 times slower than that of **6b** and is about seven times faster at temperatures below 180 K. The lifetime of the unidentified intermediate **7b** is about 400 times longer than that of singlet nitrene **3Sb** in fluid solution at ambient temperature. Moreover, the lifetime of this intermediate does not depend on deuteration and is not shortened in the presence of water and alcohol. At this time, the only tentative assignment of the intermediate **7b** is to a complex between the nitrene and the pendant phenyl ring. More calculations and experiments must be performed to support or exclude this assignment.

All experimental results are in excellent agreement with CASPT2 and density functional theoretical calculations.

## Acknowledgements

Support of this work in Columbus by the National Science Foundation and by the Ohio Supercomputer Center is gratefully acknowledged. One of us (N.P.G.) gratefully acknowledges the support of the NSF, Ministry of Education of Russian Federation (grant E02-5.0-27) and the Division of Chemistry and Material Sciences of Russian Academy of Sciences. MLT thanks the Ohio State University for a Presidential Fellowship. The authors wish to thank Professor Bern Kohler for the use of his femtosecond pump–probe spectrometer.

## References

- 1 M.-L. Tsao, N. P. Gritsan, T. R. James, M. S. Platz, D. Hrovat and W. T. Borden, 'Study of the Chemistry of *ortho*- and *para*-Biphenylnitrenes by Laser Flash Photolysis and Time-Resolved IR Experiments and by B3LYP and CASPT2 Calculations', *J. Am. Chem. Soc.*, 2003, **125**, 9343.
- 2 (a) P. A. S. Smith and B. B. Brown, 'The reaction of aryl azides with hydrogen halides', *J. Am. Chem. Soc.*, 1951, **73**, 2438; (b) P. A. S. Smith and B. B. Brown, 'The synthesis of heterocyclic compounds from aryl azides. I. Bromo and nitro carbazoles', *J. Am. Chem. Soc.*, 1951, **73**, 2435; (c) P. A. S. Smith and J. H. Hall, 'Kinetic evidence for the formation of azene (electron-deficient nitrogen) intermediates from aryl azides', *J. Am. Chem. Soc.*, 1962, **84**, 1632; (d) P. A. S. Smith, in *Azides and Nitrenes*, ed. E. F. U. Scriven, Academic Press, 1984, p. 95; (e) P. Walker and W. A. Waters, 'Pyrolysis of organic azides: a mechanistic study', *J. Am. Chem. Soc.*, 1961, **84**, 408.
- 3 (a) R. J. Sundberg, M. Brenner, S. R. Suter and B. P. Das, 'Reactions of arylnitrenes. Bond reorganizations in *o*-biphenylnitrene and phenylnitrene', *Tetrahedron Lett.*, 1970, **31**, 2715; (b) R. J. Sundberg and R. W. Heintzelman, 'Reactivity of aryl nitrenes. Competition between carbazole formation and internal bond reorganization in biphenylnitrenes', *J. Org. Chem.*, 1974, **39**, 2546; (c) R. J. Sundberg, D. W. Gillespie and B. A. DeGraff, 'Mechanism of photolytic conversion of 2-azidobiphenyl to carbazole', *J. Am. Chem. Soc.*, 1975, **97**, 6193.
- 4 (a) R. J. Sundberg, S. R. Suter and M. Brenner, 'Photolysis of *o*-substituted aryl azides in diethylamine. Formation and autoxidation of 2-diethylamino-1H-azepine intermediates', *J. Am. Chem. Soc.*, 1972, **94**, 513; (b) E. Leyva and R. Sagredo, 'Photochemistry of fluorophenyl azides in diethylamine. Nitrene reaction *versus* ring expansion', *Tetrahedron*, 1998, **54**, 736.
- 5 (a) N. P. Gritsan, A. D. Gudmundsdóttir, D. Tigelaar and M. S. Platz, 'Laser flash photolysis study of methyl derivatives of phenyl azide', *J. Phys. Chem. A*, 1999, **103**, 3458; (b) N. P. Gritsan, A. D. Gudmundsdóttir, D. Tigelaar, Z. Zhu, W. L. Karney, C. M. Hadad and M. S. Platz, 'A laser flash photolysis and quantum chemical study of the fluorinated derivatives of singlet phenylnitrene', *J. Am. Chem. Soc.*, 2001, **123**, 1951; (c) N. P. Gritsan and M. S. Platz, 'Kinetics and spectroscopy of substituted phenylnitrenes', *Adv. Phys. Org. Chem.*, 2001, **36**, 255.
- 6 C. B. Martin, X. Shi, M.-L. Tsao, D. Karweik, J. Brooke, C. M. Hadad and M. S. Platz, 'The Photochemistry of Riboflavin Tetraacetate and Nucleosides. A Study Using Density Functional Theory, Laser Flash Photolysis, Fluorescence, UV-Vis, and Time Resolved Infrared Spectroscopy', *J. Phys. Chem. B*, 2002, **106**, 10263.

- 7 J. Peon, G. C. Hess, J.-M. L. Pecourt, T. Yuzawa and B. Kohler, 'Ultrafast Photoionization Dynamics of Indole in Water', *J. Phys. Chem. A*, 1999, **103**, 2460.
- 8 (a) B. O. Roos, in *Ab Initio Methods in Quantum Chemistry*, ed. K. P. Lawley, Wiley: New York, 1987, vol. 2, p. 399; (b) B. O. Roos, 'The complete active space self-consistent field method and its applications in electronic structure calculations', *Adv. Chem. Phys.*, 1987, **69**, 399; (c) B. O. Roos, 'The complete active space SCF method in a Fock-Matrix-based super-CI formulation', *Int. J. Quant. Chem. Symp.*, 1980, **14**, 175.
- 9 P. C. Hariharan and J. A. Pople, 'Influence of polarization functions on MO hydrogenation energies', *Theor. Chim. Acta*, 1973, **28**, 213.
- 10 W. L. Karney and W. T. Borden, 'Ab Initio Study of the Ring Expansion of Phenylnitrene and Comparison with the Ring Expansion of Phenylcarbene', *J. Am. Chem. Soc.*, 1997, **119**, 1378.
- 11 (a) K. Anderson, P.-Å. Malmqvist, B. O. Roos, A. J. Sadlej and K. Wolinski, 'Second-order perturbation theory with a CASSCF reference function', *J. Phys. Chem.*, 1990, **94**, 5483; (b) K. Anderson, P.-Å. Malmqvist and B. O. Roos, 'Second-order perturbation theory with a complete active space self-consistent field reference function', *J. Chem. Phys.*, 1992, **96**, 1218; (c) K. Anderson and B. O. Roos, 'Multiconfigurational second-order perturbation theory: a test of geometries and binding energies', *Int. J. Quant. Chem.*, 1993, **45**, 591.
- 12 B. O. Roos, K. Anderson, M. P. Fulscher, L. Serrano-Andres, K. Pierloot, M. Merchank and V. Molinac, 'Application of level shift corrected perturbation theory in electronic spectroscopy', *J. Mol. Struct. (THEOCHEM)*, 1996, **388**, 257.
- 13 K. Andersson, M. Barysz, A. Bernhardsson, M. R. A. Blomberg, D. L. Cooper, T. Fleig, M. P. Fulscher, C. de Graaf, B. A. Hess, G. Karlström, R. Lindh, P.-Å. Malmqvist, P. Neogrády, J. Olsen, B. O. Roos, A. J. Sadlej, M. Schütz, B. Schimmelpfennig, L. Seijo, L. Serrano-Andrés, P. E. M. Siegbahn, J. Stålring, T. Thorsteinsson, V. Veryazov and P.-O. Widmark, *MOLCAS, Version 5*, Lund University, Sweden, 2000.
- 14 (a) A. D. Becke, 'Density-functional thermochemistry. III. The role of exact exchange', *J. Chem. Phys.*, 1993, **98**, 5648; (b) C. Lee and W. Yang, R. G. Parr, 'Development of the Colle-Salvetti correlation-energy formula into a functional of the electron density', *Phys. Rev. B*, 1988, **37**, 785; (c) B. Miehlich, A. Savin, H. Stoll and H. Preuss, 'Results obtained with the correlation energy density functionals of Becke and Lee, Yang and Parr', *Chem. Phys. Lett.*, 1989, **157**, 200.
- 15 (a) M. J. Frisch, J. A. Pople and J. S. Binkley, 'Self-consistent molecular orbital methods. 25. Supplementary functions for Gaussian basis sets', *J. Chem. Phys.*, 1984, **80**, 3265; (b) T. Clark, J. Chandrasekhar and P. v. R. Schleyer, 'Efficient diffuse function-augmented basis sets for anion calculations. III. The 3-21+G basis set for first-row elements, lithium to fluorine', *J. Comp. Chem.*, 1983, **4**, 294.
- 16 M. E. Casida, C. Jamorski, K. C. Casida and D. R. Salahub, 'Molecular excitation energies to high-lying bound states from time-dependent density-functional response theory: characterization and correction of the time-dependent local density approximation ionization threshold', *J. Chem. Phys.*, 1998, **108**, 4439.
- 17 M. J. Frisch, G. W. Trucks, H. B. Schlegel, G. E. Scuseria, M. A. Robb, J. R. Cheeseman, V. G. Zakrzewski, J. A. Montgomery, Jr., R. E. Stratmann, J. C. Burant, S. Dapprich, J. M. Millam, A. D. Daniels, K. N. Kudin, M. C. Strain, O. Farkas, J. Tomasi, V. Barone, M. Cossi, R. Cammi, B. Mennucci, C. Pomelli, C. Adamo, S. Clifford, J. Ochterski, G. A. Petersson, P. Y. Ayala, Q. Cui, K. Morokuma, D. K. Malick, A. D. Rabuck, K. Raghavachari, J. B. Foresman, J. Cioslowski, J. V. Ortiz, B. B. Stefanov, G. Liu, A. Liashenko, P. Piskorz, I. Komaromi, R. Gomperts, R. L. Martin, D. J. Fox, T. Keith, M. A. Al-Laham, C. Y. Peng, A. Nanayakkara, C. Gonzalez, M. Challacombe, P. M. W. Gill, B. G. Johnson, W. Chen, M. W. Wong, J. L. Andres, M. Head-Gordon, E. S. Replogle and J. A. Pople, *GAUSSIAN 98 (Revision A.9)*, Gaussian, Inc., Pittsburgh, PA, 1998.
- 18 M.-L. Tsao and M. S. Platz, 'Photochemistry of *Ortho*, *Ortho*' Dialkyl Phenyl Azides', *J. Am. Chem. Soc.*, 2003, **125**, 12014.
- 19 (a) S. A. Kovalenko, R. Schanz, H. Hennig and N. P. Ernsting, 'Cooling dynamics of an optically excited molecular probe in solution from femtosecond broadband transient absorption spectroscopy', *J. Chem. Phys.*, 2001, **115**, 3256; (b) R. Knochenmuss, V. Karbach, C. Wickleder, S. Graf and S. Leutwyler, 'Vibrational-energy redistribution and vibronic coupling in 1-naphthol×water complexes', *J. Phys. Chem. A*, 1998, **102**, 1935; (c) V. Wong and M. Gruebele, 'How Does Vibrational Energy Flow Fill the Molecular State Space?', *J. Phys. Chem. A*, 1999, **103**, 10664; (d) N. E. Levinger, P. H. Davis and M. D. Fayer, 'Vibrational relaxation of the free terminal hydroxyl stretch in methanol oligomers: Indirect pathway to hydrogen bond breaking', *J. Chem. Phys.*, 2001, **115**, 9352; (e) M. Gruebele, 'Vibrational energy flow: a state space approach', *Adv. Chem. Phys.*, 2001, **114**, 193.
- 20 N. P. Gritsan and M. S. Platz, unpublished results.